

Brain Topography

Ipsilateral alteration of resting state activity suggest that cortical dysfunction contributes to the pathogenesis of cluster headache

--Manuscript Draft--

Manuscript Number:	BTOP-D-16-00010R1
Full Title:	Ipsilateral alteration of resting state activity suggest that cortical dysfunction contributes to the pathogenesis of cluster headache
Article Type:	Original Article
Section/Category:	Clinical applications
Keywords:	cluster headache; MRI; frequency analysis; resting state networks; dual regression
Corresponding Author:	Kincses Zsigmond Tamás, MD, PhD Department of Neurology, University of Szeged Szeged, HUNGARY
Corresponding Author Secondary Information:	
Corresponding Author's Institution:	Department of Neurology, University of Szeged
Corresponding Author's Secondary Institution:	
First Author:	Péter Faragó, MD
First Author Secondary Information:	
Order of Authors:	Péter Faragó, MD Eszter Tóth, MD András Király, MD Nikoletta Szabó, MD, PhD Gergő Csete, MD Bernadett Tuka, PhD Csaba Ertsey, MD, PhD Délia Szok, MD János Tajti, MD Árpád Párdutz László Vécsei, MD, PhD, DSc Kincses Zsigmond Tamás, MD, PhD
Order of Authors Secondary Information:	
Funding Information:	
Abstract:	<p>Background: The pathomechanism of cluster headache (CH) is not entirely understood, but central and peripheral components were suggested. A recent report showed that transcranial magnetic stimulation measured cortical excitability was increased in the hemisphere ipsilateral to the pain. In the current study we set out to investigate the amplitude of resting brain fMRI activity to find signatures of the increased excitability.</p> <p>Methods: High resolution T1 weighted and resting state functional MRI images were acquired from seventeen patients with CH in pain free period and from twenty-six healthy volunteers. Patients' data were normalized (e.g. inverted along the midsagittal axis) according to the headache side. Independent component analysis and a modified dual regression approach were used to reveal the differences between the resting state networks. Furthermore, the timecourses were decomposed into five frequency</p>

bands by discrete wavelet decomposition and were also re-regressed to the original data to reveal frequency specific resting activity maps.

Results: Two of the identified resting state networks showed alterations in CH. When the data were inverted to have patients' headaches on the left, the ipsilateral attention network showed increased connectivity in 0.08-0.04 Hz frequency band in the in CH group. In the same dataset, cerebellar network showed higher functional connectivity in 0.02-0.01 Hz range in the ipsilateral cerebellum. When the data of patients having headache on the left were inverted to the right, similar increased signal was found in the ipsilateral attention network in 0.08-0.04Hz band. The cerebellar network showed increased connectivity in the cerebellum in 0.02-0.01 Hz band in patients. The Fourier analysis of these area revealed increased power in CH at all cases.

Conclusions: Our results showed alterations of brain functional networks in CH. The alterations of resting state activity were found in the hemisphere ipsilateral to the pain, signifying the altered cortical processing in the pathomechanism of CH.

[Click here to view linked References](#)

Ipsilateral alteration of resting state activity suggests that cortical dysfunction contributes to the pathogenesis of cluster headache

Péter Faragó¹, Nikoletta Szabó^{1,2}, Eszter Tóth¹, Bernadett Tuka¹, András Király¹, Gergő Csete¹, Árpád Párdutz¹, Délia Szok¹, János Tajti¹, Csaba Ertsey³, László Vécsei^{1,4}, Zsigmond Tamás Kincses^{1,2}

¹Department of Neurology, Faculty of General Medicine, University of Szeged, Szeged, Hungary

²International Clinical Research Center, St. Anne's University Hospital Brno, Brno, Czech Republic

³Department of Neurology, Semmelweis University, Budapest, Hungary

⁴MTA-SZTE Neuroscience Research Group, Szeged, Hungary

Keywords: cluster headache, MRI, resting state networks, dual regression, frequency analysis

Corresponding author:

Dr. Zsigmond Tamás Kincses

Department of Neurology

Albert Szent-György Clinical Center

University of Szeged

Semmelweis u. 6

6724 - Szeged

Hungary

Email.: kincses.zsigmond.tamas@med.u-szeged.hu

Abstract

Background: The pathomechanism of cluster headache (CH) is not entirely understood, but central and peripheral components were suggested. A recent report showed that transcranial magnetic stimulation measured cortical excitability was increased in the hemisphere ipsilateral to the pain. In the current study we set out to investigate the amplitude of resting brain fMRI activity to find signatures of the increased excitability.

Methods: High resolution T1 weighted and resting state functional MRI images were acquired from seventeen patients with CH in pain free period and from twenty-six healthy volunteers. Patients' data were normalized (e.g. inverted along the midsagittal axis) according to the headache side. Independent component analysis and a modified dual regression approach were used to reveal the differences between the resting state networks. Furthermore, the timecourses were decomposed into five frequency bands by discrete wavelet decomposition and were also re-regressed to the original data to reveal frequency specific resting activity maps.

Results: Two of the identified resting state networks showed alterations in CH. When the data were inverted to have patients' headaches on the left, the ipsilateral attention network showed increased connectivity in 0.08-0.04 Hz frequency band in the in CH group. In the same dataset, cerebellar network showed higher functional connectivity in 0.02-0.01 Hz range in the ipsilateral cerebellum. When the data of patients having headache on the left were inverted to the right, similar increased signal was found in the ipsilateral attention network in 0.08-0.04Hz band. The cerebellar network showed increased connectivity in the cerebellum in 0.02-0.01 Hz band in patients. The Fourier analysis of these area revealed increased power in CH at all cases.

Conclusions: Our results showed alterations of brain functional networks in CH. The alterations of resting state activity were found in the hemisphere ipsilateral to the pain, signifying the altered cortical processing in the pathomechanism of CH.

1
2
3
4
5
6
7
8
9
10
11
12
13
14
15
16
17
18
19
20
21
22
23
24
25
26
27
28
29
30
31
32
33
34
35
36
37
38
39
40
41
42
43
44
45
46
47
48
49
50
51
52
53
54
55
56
57
58
59
60
61
62
63
64
65

Introduction

Cluster headache (CH) is one of the most painful primary headache disorders. The disease is characterized by severe, strictly unilateral, retro-orbital pain with ipsilateral autonomic symptoms, such as lacrimation, rhinorrhea, conjunctival injection (Headache Classification Committee of the International Headache 2013). These attacks usually appear on a daily basis for a period lasting several weeks or months (the cluster period), followed by lengthy headache-free periods. The cluster periods notably follow a circadian pattern. While there are some effective possibilities for acute treatment of attacks, a highly effective preventative measure is missing.

Imaging studies provided several clues about the disease. Structural imaging studies revealed, the total gray matter volume was decreased in CH patients compared to healthy controls in the frontal lobe in interictal period (Yang et al. 2013). We and others showed that there is an extensive white matter microstructural alteration in the pain free period in CH (Szabo et al. 2013; Teepker et al. 2012).

Functional imaging studies showed higher activation in the ipsilateral hypothalamus during attacks with positron emission tomography (May et al. 1998) and functional MRI (May et al. 2000; Morelli et al. 2009; Sprenger et al. 2004). Furthermore, altered functional connectivity of the hypothalamus and anterior thalamus were also described (Qiu et al. 2015; Qiu et al. 2013; Rocca et al. 2010; Yang et al. 2014). Moreover, the activity of the pain matrix (e.g. according to Tracey: „large distributed brain network [activating] during nociceptive processing” (Tracey 2008)) and the connectivity to some of its structures were found to be altered too (Sprenger et al. 2007; Yang et al. 2014).

The alteration of the functional connectivity between certain nodes or the expression of spatially distributed functional networks can be deciphered from the resting state

1 functional MRI (Beckmann et al. 2005b; Fox and Raichle 2007). The alterations of
2 these functional networks were shown in several diseases such as multiple sclerosis
3 (Roosendaal et al. 2010), migraine (Xue et al. 2012) or Alzheimer's disease (Greicius
4 et al. 2004). Most of the approaches analyzing the resting state BOLD fluctuations
5 focus on the correlated activity in various brain regions or search for spatially
6 independent common temporal characteristics in the fMRI data. The information in the
7 amplitude and the frequency of these resting activity fluctuations only recently came
8 into the focus of attention (Kublbock et al. 2014; Zou et al. 2008). However, none of
9 the previous studies examined alterations between the resting state networks' power
10 and their relation to the pain matrix in cluster headache. The in depth analysis of such
11 information of the resting state fluctuation is especially important in the view of recent
12 researches showing an increased cortical excitability in CH (Cosentino et al. 2015)
13 similar to that in migraine (Chadaide et al. 2007). While there is no direct evidence that
14 various parameters of TMS measured cortical excitability are represented as a variation
15 in the amplitude or the frequency of the resting BOLD fluctuations, one might speculate
16 that they are strongly related and both depict important features of cortical function.
17
18 In this study we set out to investigate resting state fMRI networks in cluster headache
19 patients in the pain free period with a special attention to the amplitude of the resting
20 activity in various frequency bands. According to our hypothesis, an altered resting
21 activity might be responsible for the development of pain, or alternatively repeated pain
22 bouts may cause maladaptive plastic changes in the brain that can be detected in the
23 resting functional connectivity and also in the local brain activity. Furthermore, these
24 changes can potentially be linked to clinical data, such as disease duration or cumulative
25 headache days.

Methods

Participants

Seventeen patients with episodic CH were recruited to this study from the Headache Outpatients Clinics of the University of Szeged and Semmelweis University. The diagnosis of the CH was made according to the International Classification of Headache Disorders. The participants had no history of any other neurological or psychiatric disorders. None of the participants used prophylactic interval therapy. The MRI scans were acquired at least 1 month after the last headache episode. Clinical variables, such as disease duration, time between bouts and average length of bouts was recorded for all patients. Furthermore, cumulative headache days was estimated for all patients that is the total number of days the patient had experienced headache over his/her entire life.

Twenty-six age and sex matched healthy individuals were recruited as a control group. All participants were right handed. The demographic data is depicted in *Table 1*. The study was approved by the ethics committee of the University of Szeged and all study participants gave written informed consent in accordance with the Declaration of Helsinki (authority number: 56/2011).

Image acquisition

The MR imaging was performed on a 1.5T GE Signa Excite HDxt MRI Scanner (Milwaukee, WI, USA). The head motion was restricted with foam padding around the head and the noise of the scanner was attenuated with earplugs. For every participant high resolution T1 weighted images (3D IR-FSPGR: TR/TE/TI: 10.3/4.2/450ms, flip angle: 15°, ASSET: 2, FOV: 25*25 cm, matrix: 256*256, slice thickness: 1mm) and a resting state fMRI protocol with echo-planar imaging technique (TE: 40 ms, TR: 300

1 ms, matrix: 64*64 cm, FOV: 30*30 cm, slice thickness: 6 mm, flip angle: 90°, NEX: 1,
2 ASSET: 2,0 Ph, Phases per Loc: 128, volumes: 200) were acquired. Subjects were
3
4 asked to stay awake during the acquisition and lay in the scanner with closed eyes.
5
6

7 8 **Data preprocessing** 9

10
11 All image processing was carried out with the algorithms in FMRIB's Software Library
12 (<http://www.fmrib.ox.uk/fsl>, Oxford, UK). Since in CH the headache is strictly
13 unilateral, according to the literature (Absinta et al. 2012; Szabo et al. 2013; Yang et al.
14 2014), we normalized the data according to the headache side: the images of patients
15 having headache on the left side were inverted along the midsagittal axis by the
16 *fslswapdim* command. To acknowledge that there are non-pain related differences
17 between the left and right hemispheres we repeated the analysis by inverting the images
18 of the patients who had headache on the right side. (The analysis of the noninverted
19 data is presented in the Supplementary material.) The pre-processing was carried out
20 with FEAT (FMRI Expert Analysis Tool). The first two non steady-state volumes from
21 the 200 resting-state images were wiped out. Brain extraction (BET) was applied in all
22 structural and functional images to remove all non-brain tissues (Smith 2002). The
23 images were motion corrected by MCFLIRT and spatially smoothed with Gaussian
24 kernel of 6 mm FWHM (Jenkinson et al. 2002). A high-pass filter with cutoff sigma of
25 100 s was applied to all functional images.
26
27 Furthermore, all participants' functional images were registered to their own T1 images
28 with boundary-based registration and to a standard brain (MNI152T1) with a linear
29 registration with 12 degree of freedom using FLIRT and then a non-linear registration
30 via FSL's FNIRT (Jenkinson et al. 2002). The functional data were transformed to a
31 standard space with 4 mm resampling resolution.
32
33
34
35
36
37
38
39
40
41
42
43
44
45
46
47
48
49
50
51
52
53
54
55
56
57
58
59
60
61
62
63
64
65

Task-free network identification

Independent component analysis was used to identify the large-scale neuronal networks (Beckmann et al. 2005b). The investigation was carried out with Multivariate Exploratory Linear Optimized Decomposition into Independent Components (MELODIC) command using multi-session temporal concatenation.

The preprocessed data variance was normalized and demeaned, and then a voxel wise concatenation was applied. The resulted dataset was decomposed into a set of independent components that characterize the underlying processes in the spatial and temporal domains in such a way that spatial matrices are maximally non-Gaussian. The spatial maps of the resting state networks were thresholded to $p < 0.5$ by using Gaussian/Gamma mixture model fitting as an alternative hypothesis.

Spatio-temporal components representing artifacts, outliers and non-pain related networks were excluded from further analysis (Beckmann et al. 2005b; Qiu et al. 2013; Tian et al. 2013; Yang et al. 2014). Eight networks were subjected to further analysis: medial visual network, lateral visual network, auditory network, sensorimotor network, default mode network, salience network, ipsilateral and contralateral attention network, cerebellar network (Beckmann et al. 2005a).

Between group differences of the expression of the resting state networks

The analysis of between group differences were carried out by a modified dual regression approach (Beckmann C. F. 2009; Filippini et al. 2009). The selected networks' spatial map was thresholded at a probability greater than 0.5 and binarised. The maps were then transformed into the individuals' resting fMRI space to reveal the subject specific temporal dynamics of the networks.

1 These time courses were decomposed by discrete wavelet decomposition (see below)
2 into five frequency bands. Then the band-pass filtered timecourses were used in a linear
3 model fit (temporal regression) against the associated fMRI data to estimate subject-
4 and frequency-specific spatial maps. Finally, these spatial maps were compared across
5 groups. Modelling was accomplished using standard general linear model (GLM) setup,
6 explanatory variable coded for group membership. To examine the correlation between
7 the clinical variables and the frequency specific expression of resting state networks
8 cumulative headache days were used as a regressor in the GLM design. Statistical
9 inference was carried out by using nonparametric permutation test (5000 permutations)
10 (Nichols and Holmes 2002). Thresholding was carried out with threshold-free cluster
11 enhancement (TFCE) (Smith and Nichols 2009); the statistical results were corrected
12 for multiple comparisons. (The scheme of the modified dual regression analysis is
13 depicted in the Supplementary material.)

14 In order to restrict the dual regression analysis to specific frequency bands discrete
15 wavelet decomposition of the time courses was used to bandpass filter the data before
16 the second regression step. (Wavelet Toolbox of the Matlab software package;
17 MathWorks Inc). The discrete wavelet decomposition is an implementation of the
18 wavelet transform using a set of predefined wavelet scales and translations and
19 decomposes the signal into mutually orthogonal set of wavelets. Wavelets are brief
20 waves, they are finitely extended and their oscillations decay to zero rapidly, satisfying
21 the admissibility condition:

$$22 \int \Psi(t)dt = 0.$$

23 By dilating and translating a “mother” wavelet (Ψ) and a “father” wavelet (Φ)

$$24 \int \Phi(t)dt = 1$$

25 a wavelet family can be obtained:

$$\Psi_{jk}(t) = \frac{1}{\sqrt{2^j}} \Psi\left(\frac{t - 2^j k}{2^j}\right);$$

$$\Phi_{jk}(t) = \frac{1}{\sqrt{2^j}} \Phi\left(\frac{t - 2^j k}{2^j}\right);$$

where j is index of the scale $S_j=2^j$ and k indexes the $K=n/2^j$ location in time. The Daubechies wavelet was used as mother wavelet. The analysis by using a halfband filtering, decomposes the data over a hierarchy of scales (S_j). At each scale the data is split into two orthogonal components: details (d_{jk}) containing the high frequency information and approximations (a_{jk}) containing the low frequency information. By five levels of decomposition the following frequency bands were derived: 0-0.16 Hz: 0.16-0.08Hz, 0.08-0.04Hz, 0.04-0.02Hz, 0.02-0.01Hz and 0.01-0Hz. These decomposed, band-pass filtered timecourses were used in the modified dual regression approach (see above).

Amplitude of the resting state activity

For each subject the mean time course of every resting state network where group differences were detected with the dual regression analysis was extracted and subjected to further analysis. To investigate the amplitude of the resting activity in the different frequency bands the individual time courses of each of the subjects for the components of interest were subjected to Fourier Transformation. The power spectrums were compared between groups by two-sample t-tests and the results were corrected for multiple comparisons by Bonferoni correction.

Results

Network identification

The ICA analysis identified 30 different spatio-temporal components in the right inverted dataset and 29 in the left inverted dataset. Resting state networks revealed by previous articles showed similar distribution (Beckmann et al. 2005b; Mantini et al. 2007). Based on these articles, we selected six of these networks for further analysis: default mode network, contralateral and ipsilateral attention network, medial visual network, lateral visual network, cerebellar network.

Frequency specific expression of resting state networks

Left sided headache dataset

The dual regression analysis revealed alterations of the **ipsilateral** attention network in CH patients in two frequency bands: 0.08-0.04 Hz and 0.04-0.02 Hz. **A significantly increased degree of coactivation** within the **ipsilateral** attention network was found in the superior frontal gyrus and the medial frontal cortex ($p < 0.03$; Figure 1/a and Table 2).

A significantly increased degree of coactivation within the cerebellar network was found in CH patients in the 0.02-0.01 Hz frequency range in the **ipsilateral** cerebellar hemisphere ($p < 0.03$; Figure 1/b and Table 2).

The Fourier Transformation revealed increased power activity in patients of the **ipsilateral** attention network in the 0.04-0.07 Hz frequency band. Similarly, in the cerebellar network between 0-0.02 Hz patients showed a higher activity (Figure 1/c).

1
2
3
4
5
6
7
8
9
10
11
12
13
14
15
16
17
18
19
20
21
22
23
24
25
26
27
28
29
30
31
32
33
34
35
36
37
38
39
40
41
42
43
44
45
46
47
48
49
50
51
52
53
54
55
56
57
58
59
60
61
62
63
64
65

There were no other significant differences between the groups in other resting state networks in any other frequency bands.

Right sided headache data set

A significantly increased degree of coactivation within the ipsilateral attention network was found in patients in the 0.04-0.08Hz frequency band in the right superior frontal gyrus ($p < 0.003$) and in the right medial frontal gyrus ($p < 0.05$; Figure 2/a and Table 2).

In the cerebellar network, in the frequency range of 0.01-0.02 Hz, a significantly increased degree of coactivation was found in the contralateral cerebellum in the CH group compared to controls ($p < 0.05$; Figure 2/b and Table 2).

The power spectrum analysis showed higher activity at the ipsilateral attention network between 0.04-0.06 Hz and at the cerebellar network around 0.02 Hz (Figure 2/c).

There were no differences between the control and patient group in any other networks in any of the frequency bands.

Connection between resting state activity and clinical data

The correlation between the cumulative headache days and degree of coactivation in the resting state networks revealed significant results in one network in each dataset (right and left sided headache dataset).

The analysis of the left sided headache dataset revealed negative correlation between the cumulative headache days and the degree of coactivation in the contralateral attention network in the 0.04-0.08 Hz band in the contralateral frontal pole ($R = -0.83$, $p < 0.001$; Figure 3/a).

The analysis of the right sided headache dataset revealed negative correlation between the degree of coactivation within the contralateral attention network and the cumulative

1 number of the headache days in the 0.16-0.08 Hz frequency band in the **contralateral**
2 frontal pole ($R=-0.81$; $p<0.05$; Figure 3/b).

3
4
5 **There was no other correlation between the cumulative headache days and degree of**
6
7 **coactivation in any other resting state network. No other clinical variables showed**
8
9 **significant correlation with the measured MRI parameters.**
10

11 Discussion

12
13
14
15
16
17 Our study revealed increased frequency specific activity in CH patients in the attention
18 network ipsilateral to the headache side and in the contralateral cerebellar network. This
19 increased activity must be understood as increased frequency specific coherent activity
20 within networks and also increased amplitude of the BOLD fluctuation.
21
22

23
24
25
26
27 Former studies agreed on the altered functional connectivity of the hypothalamus in CH
28 (Qiu et al. 2015; Qiu et al. 2013; Yang et al. 2014), and also on the alteration of the
29 connectivity of other regions such as the medial frontal cortex and the cerebellum.
30
31 Similarly, Rocca and co-workers found decreased resting BOLD fluctuation in the
32 sensorimotor network in CH with some of which regions are also in the medial frontal
33 cortex (Rocca et al. 2010). Our results also pointed out the altered connectivity of the
34 medial prefrontal region. The altered resting state activity of the medial frontal cortex,
35 which is part of various resting state networks points to the key role of the medial frontal
36 cortex in the pain perception or in the pathogenesis of CH.
37
38

39
40
41
42
43
44
45
46
47
48
49 Our results also fit well into our current knowledge about CH, hypothalamus being a
50 key component of the pathomechanism. The anteroventral compartment of the
51 hypothalamus was shown to be connected predominantly with the prefrontal cortex and
52 the dorsal supplementary motor area in a diffusion tractography study (Lemaire et al.
53
54
55
56
57
58
59
60
61
62
63
64
65

1997). On the other hand cerebellar connection of the hypothalamus was also revealed in humans (Lemaire et al. 2011) and in animal studies (Dietrichs and Haines 2002). Moreover the effective site of the deep brain stimulation for CH in the ipsilateral hypothalamus was shown to have high probability connectivity to the medial lemniscus, frontal cortex and to the cerebellum (Owen et al. 2007).

Furthermore, the frontal regions that showed altered resting BOLD fluctuations are very much alike to some of the regions showing atrophy in CH (Absinta et al. 2012; Naegel et al. 2014). Furthermore, the disorganized connectivity could be a result of white matter microstructural alteration that we have described in CH earlier (Szabo et al. 2013).

We also found a higher amplitude activity in patients in areas where we found higher connectivity. Former studies investigated the amplitude of the resting state fluctuation in diseases with chronic pain (Baliki et al. 2014; Malinen et al. 2010b). Baliki and colleagues found increased amplitude of activity in the default mode network in patients with chronic pain. The alterations were found predominantly in the higher frequencies. This article also describes increased amplitude of BOLD activity in a pain related network and in the cerebellum.

One important aspect of our results is that the medial frontal activity differences were in the attention network ipsilateral to the headache side, a result coincide with former transcranial magnetic stimulation study showing increased cortical excitability ipsilateral to the pain in CH (Cosentino et al. 2015). While several studies indicated the important role of the hypothalamus in CH (May et al. 1998; May et al. 2000; Morelli et al. 2009; Qiu et al. 2015; Qiu et al. 2013; Rocca et al. 2010; Sprenger et al. 2004; Yang et al. 2014), it is still debated if it actively contributes to the attacks or the altered hypothalamic activation is secondary to the cortical and subcortical malfunction of the

1 pain matrix. The primary role of the cortical dysfunction was strengthened by former
2 electrophysiological studies (Casale et al. 2008; van Vliet et al. 2003) and the existence
3
4 of aura symptoms before the pain also point to this direction. The increased cortical
5 excitability (Cosentino et al. 2015) might present in an increased amplitude of BOLD
6
7 fluctuation-and might lead to the changes of various transmitter levels that activates the
8
9 trigeminal endings such as in migraine (Tajti et al. 2015; Tuka et al. 2013).
10
11

12
13
14 Incontrast to the ipsilateral functional alterations found in the current investigation,
15
16 microstructural alterations in our previous DTI study were somewhat lateralized to the
17
18 hemisphere contralateral to the headache (Szabo et al. 2013) suggesting chronic
19
20 microstructural alterations, which we believe is a kind of a disintegration of the white
21
22 matter due to the recurring painful attacks.
23
24

25
26 Recently, the focus of attention has shifted to investigate the activity of resting state
27
28 fluctuations in various frequency bands (Gao et al. 2015), especially in pain conditions
29
30 (Kim et al. 2013; Otti et al. 2013). The importance of the various frequencies of BOLD
31
32 fluctuations is not yet known. It was proposed that functional connectivity of various
33
34 brain regions are represented in different dominant frequency bands (Salvador et al.
35
36 2008). This could be responsible for the alterations found in different frequency bands
37
38 in the attention network and the cerebellar network. Another option might be that CH
39
40 was proposed to be a neurovascular disease, and the altered neurovascular coupling
41
42 may affect the frequency of the resting BOLD fluctuations (Malinen et al. 2010a;
43
44 Malinen et al. 2010b) by acting as a filter. Furthermore, the group difference in the
45
46 resting state network activity might well be the result of improved signal to noise ratio
47
48 by filtering out the low and high frequency artifact. Since most of the slow frequency
49
50 fluctuation in our analysis with a relatively long TR were shown to be neural origin
51
52 (Boyacioglu et al. 2013), this hypothesis seems rather unlikely.
53
54
55
56
57
58
59
60
61
62
63
64
65

Conclusion

We propose that the altered resting state activity on the side of headache that might be a signature of increased cortical excitability may play an important role in the pathogenesis of CH.

Conflict of interest

The authors declare that there are no conflicts of interest.

Acknowledgement

The study was supported by the „Neuroscience Research Group of the Hungarian Academy of Sciences and University of Szeged”, project FNUSA-ICRC (no. CZ.1.05/1.1.00/02.0123) from the European Regional Development Fund, the National Brain Research Program (Grant No. KTIA_13_NAP-A-II/20.) and an OTKA [PD 104715] grant. Dr. Szabó and Dr. Kincses were supported by European Regional Development Fund - Project FNUSA-ICRC (No. CZ.1.05/1.1.00/02.0123) and by European Union - project ICRC-ERA-HumanBridge (No. 316345). Dr. Párdutz was supported by the Bolyai Scholarship Program of the Hungarian Academy of Sciences.

References

- 1
2
3 Absinta M, Rocca MA, Colombo B, Falini A, Comi G, Filippi M (2012) Selective
4 decreased grey matter volume of the pain-matrix network in cluster headache
5
6 Cephalalgia : an international journal of headache 32:109-115
7
8 doi:10.1177/0333102411431334
9
10
11
12 Baliki MN, Mansour AR, Baria AT, Apkarian AV (2014) Functional Reorganization
13 of the Default Mode Network across Chronic Pain Conditions PloS one 9 doi:ARTN
14
15 e106133
16
17 10.1371/journal.pone.0106133
18
19
20
21 Beckmann C. F. FN, Smith S.M. (2009) Group comparison of resting-state fMRI data
22 using multi-subject ICA and dual regression. NeuroImage 47:S39-S41
23
24
25 Beckmann CF, DeLuca M, Devlin JT, Smith SM (2005a) Investigations into resting-
26 state connectivity using independent component analysis Philos Trans R Soc Lond B
27
28 Biol Sci 360:1001-1013 doi:10.1098/rstb.2005.1634
29
30
31
32 Beckmann CF, DeLuca M, Devlin JT, Smith SM (2005b) Investigations into resting-
33 state connectivity using independent component analysis Philos T Roy Soc B
34
35 360:1001-1013 doi:Doi 10.1098/Rstb.2005.1634
36
37
38
39 Boyacioglu R, Beckmann CF, Barth M (2013) An Investigation of RSN Frequency
40 Spectra Using Ultra-Fast Generalized Inverse Imaging Frontiers in human neuroscience
41
42 7:156 doi:10.3389/fnhum.2013.00156
43
44
45
46 Casale MS, Baratto M, Cervera C, Gallamini M, Lynch G, Gjini K, Boutros NN (2008)
47
48 Auditory evoked potential abnormalities in cluster headache Neuroreport 19:1633-
49
50 1636 doi:10.1097/WNR.0b013e328314e0dd
51
52
53
54
55
56
57
58
59
60
61
62
63
64
65

1 Chadaide Z, Arlt S, Antal A, Nitsche MA, Lang N, Paulus W (2007) Transcranial direct
2 current stimulation reveals inhibitory deficiency in migraine Cephalalgia 27:833-839
3
4 doi:10.1111/j.1468-2982.2007.01337.x
5
6

7 Cosentino G, Brighina F, Brancato S, Valentino F, Indovino S, Fierro B (2015)
8
9 Transcranial magnetic stimulation reveals cortical hyperexcitability in episodic cluster
10 headache J Pain 16:53-59 doi:10.1016/j.jpain.2014.10.006
11
12

13
14 Dietrichs E, Haines DE (2002) Possible pathways for cerebellar modulation of
15 autonomic responses: micturition Scandinavian journal of urology and nephrology
16 Supplementum:16-20
17
18

19
20
21
22 Filippini N et al. (2009) Distinct patterns of brain activity in young carriers of the
23 APOE-epsilon4 allele Proc Natl Acad Sci U S A 106:7209-7214
24
25
26
27 doi:10.1073/pnas.0811879106
28

29
30 Fox MD, Raichle ME (2007) Spontaneous fluctuations in brain activity observed with
31 functional magnetic resonance imaging Nature reviews Neuroscience 8:700-711
32
33
34
35 doi:10.1038/nrn2201

36
37 Gao L et al. (2015) Frequency-dependent changes of local resting oscillations in sleep-
38 deprived brain PloS one 10:e0120323 doi:10.1371/journal.pone.0120323
39

40
41 Greicius MD, Srivastava G, Reiss AL, Menon V (2004) Default-mode network activity
42 distinguishes Alzheimer's disease from healthy aging: evidence from functional MRI
43
44
45
46
47
48
49
50
51
52
53
54
55
56
57
58
59
60
61
62
63
64
65
66
67
68
69
70
71
72
73
74
75
76
77
78
79
80
81
82
83
84
85
86
87
88
89
90
91
92
93
94
95
96
97
98
99
100
101
102
103
104
105
106
107
108
109
110
111
112
113
114
115
116
117
118
119
120
121
122
123
124
125
126
127
128
129
130
131
132
133
134
135
136
137
138
139
140
141
142
143
144
145
146
147
148
149
150
151
152
153
154
155
156
157
158
159
160
161
162
163
164
165
166
167
168
169
170
171
172
173
174
175
176
177
178
179
180
181
182
183
184
185
186
187
188
189
190
191
192
193
194
195
196
197
198
199
200
201
202
203
204
205
206
207
208
209
210
211
212
213
214
215
216
217
218
219
220
221
222
223
224
225
226
227
228
229
230
231
232
233
234
235
236
237
238
239
240
241
242
243
244
245
246
247
248
249
250
251
252
253
254
255
256
257
258
259
260
261
262
263
264
265
266
267
268
269
270
271
272
273
274
275
276
277
278
279
280
281
282
283
284
285
286
287
288
289
290
291
292
293
294
295
296
297
298
299
300
301
302
303
304
305
306
307
308
309
310
311
312
313
314
315
316
317
318
319
320
321
322
323
324
325
326
327
328
329
330
331
332
333
334
335
336
337
338
339
340
341
342
343
344
345
346
347
348
349
350
351
352
353
354
355
356
357
358
359
360
361
362
363
364
365
366
367
368
369
370
371
372
373
374
375
376
377
378
379
380
381
382
383
384
385
386
387
388
389
390
391
392
393
394
395
396
397
398
399
400
401
402
403
404
405
406
407
408
409
410
411
412
413
414
415
416
417
418
419
420
421
422
423
424
425
426
427
428
429
430
431
432
433
434
435
436
437
438
439
440
441
442
443
444
445
446
447
448
449
450
451
452
453
454
455
456
457
458
459
460
461
462
463
464
465
466
467
468
469
470
471
472
473
474
475
476
477
478
479
480
481
482
483
484
485
486
487
488
489
490
491
492
493
494
495
496
497
498
499
500
501
502
503
504
505
506
507
508
509
510
511
512
513
514
515
516
517
518
519
520
521
522
523
524
525
526
527
528
529
530
531
532
533
534
535
536
537
538
539
540
541
542
543
544
545
546
547
548
549
550
551
552
553
554
555
556
557
558
559
560
561
562
563
564
565
566
567
568
569
570
571
572
573
574
575
576
577
578
579
580
581
582
583
584
585
586
587
588
589
590
591
592
593
594
595
596
597
598
599
600
601
602
603
604
605
606
607
608
609
610
611
612
613
614
615
616
617
618
619
620
621
622
623
624
625
626
627
628
629
630
631
632
633
634
635
636
637
638
639
640
641
642
643
644
645
646
647
648
649
650
651
652
653
654
655
656
657
658
659
660
661
662
663
664
665
666
667
668
669
670
671
672
673
674
675
676
677
678
679
680
681
682
683
684
685
686
687
688
689
690
691
692
693
694
695
696
697
698
699
700
701
702
703
704
705
706
707
708
709
710
711
712
713
714
715
716
717
718
719
720
721
722
723
724
725
726
727
728
729
730
731
732
733
734
735
736
737
738
739
740
741
742
743
744
745
746
747
748
749
750
751
752
753
754
755
756
757
758
759
760
761
762
763
764
765
766
767
768
769
770
771
772
773
774
775
776
777
778
779
780
781
782
783
784
785
786
787
788
789
790
791
792
793
794
795
796
797
798
799
800
801
802
803
804
805
806
807
808
809
810
811
812
813
814
815
816
817
818
819
820
821
822
823
824
825
826
827
828
829
830
831
832
833
834
835
836
837
838
839
840
841
842
843
844
845
846
847
848
849
850
851
852
853
854
855
856
857
858
859
860
861
862
863
864
865
866
867
868
869
870
871
872
873
874
875
876
877
878
879
880
881
882
883
884
885
886
887
888
889
890
891
892
893
894
895
896
897
898
899
900
901
902
903
904
905
906
907
908
909
910
911
912
913
914
915
916
917
918
919
920
921
922
923
924
925
926
927
928
929
930
931
932
933
934
935
936
937
938
939
940
941
942
943
944
945
946
947
948
949
950
951
952
953
954
955
956
957
958
959
960
961
962
963
964
965
966
967
968
969
970
971
972
973
974
975
976
977
978
979
980
981
982
983
984
985
986
987
988
989
990
991
992
993
994
995
996
997
998
999
1000

1 Jenkinson M, Bannister P, Brady M, Smith S (2002) Improved optimization for the
2 robust and accurate linear registration and motion correction of brain images
3
4 NeuroImage 17:825-841
5

6
7 Kim JY et al. (2013) Increased power spectral density in resting-state pain-related brain
8 networks in fibromyalgia Pain 154:1792-1797 doi:10.1016/j.pain.2013.05.040
9

10
11 Kublbock M et al. (2014) Stability of low-frequency fluctuation amplitudes in
12 prolonged resting-state fMRI NeuroImage 103C:249-257
13
14 doi:10.1016/j.neuroimage.2014.09.038
15
16

17
18 Lemaire JJ et al. (2011) White matter connectivity of human hypothalamus Brain
19 research 1371:43-64 doi:10.1016/j.brainres.2010.11.072
20
21

22
23 Malinen S et al. (2010a) Aberrant temporal and spatial brain activity during rest in
24 patients with chronic pain Proceedings of the National Academy of Sciences of the
25 United States of America 107:6493-6497 doi:10.1073/pnas.1001504107
26
27

28
29 Malinen S et al. (2010b) Aberrant temporal and spatial brain activity during rest in
30 patients with chronic pain Proceedings of the National Academy of Sciences of the
31 United States of America 107:6493-6497 doi:10.1073/pnas.1001504107
32
33

34
35 Mantini D, Perrucci MG, Del Gratta C, Romani GL, Corbetta M (2007)
36 Electrophysiological signatures of resting state networks in the human brain
37 Proceedings of the National Academy of Sciences of the United States of America
38 104:13170-13175 doi:10.1073/pnas.0700668104
39
40

41
42 May A, Bahra A, Buchel C, Frackowiak RS, Goadsby PJ (1998) Hypothalamic
43 activation in cluster headache attacks Lancet 352:275-278 doi:10.1016/S0140-
44 6736(98)02470-2
45
46

47
48 May A, Bahra A, Buchel C, Frackowiak RS, Goadsby PJ (2000) PET and MRA
49 findings in cluster headache and MRA in experimental pain Neurology 55:1328-1335
50
51
52
53
54
55

1 Morelli N, Pesaresi I, Cafforio G, Maluccio MR, Gori S, Di Salle F, Murri L (2009)
2 Functional magnetic resonance imaging in episodic cluster headache The journal of
3 headache and pain 10:11-14 doi:10.1007/s10194-008-0085-z
4
5
6 Naegel S, Holle D, Desmarattes N, Theysohn N, Diener HC, Katsarava Z, Obermann
7 M (2014) Cortical plasticity in episodic and chronic cluster headache NeuroImage
8 Clinical 6:415-423 doi:10.1016/j.nicl.2014.10.003
9
10
11
12
13
14
15
16
17
18
19
20
21
22
23
24
25
26
27
28
29
30
31
32
33
34
35
36
37
38
39
40
41
42
43
44
45
46
47
48
49
50
51
52
53
54
55
56
57
58
59
60
61
62
63
64
65

Nichols TE, Holmes AP (2002) Nonparametric permutation tests for functional neuroimaging: A primer with examples Hum Brain Mapp 15:1-25 doi:Doi 10.1002/Hbm.1058

Otti A, Guendel H, Wohlschlager A, Zimmer C, Noll-Hussong M (2013) Frequency shifts in the anterior default mode network and the salience network in chronic pain disorder BMC psychiatry 13:84 doi:10.1186/1471-244X-13-84

Owen SL et al. (2007) Connectivity of an effective hypothalamic surgical target for cluster headache Journal of clinical neuroscience : official journal of the Neurosurgical Society of Australasia 14:955-960 doi:10.1016/j.jocn.2006.07.012

Qiu E, Tian L, Wang Y, Ma L, Yu S (2015) Abnormal coactivation of the hypothalamus and salience network in patients with cluster headache Neurology doi:10.1212/WNL.0000000000001442

Qiu E et al. (2013) Abnormal brain functional connectivity of the hypothalamus in cluster headaches PloS one 8:e57896 doi:10.1371/journal.pone.0057896

Risold PY, Thompson RH, Swanson LW (1997) The structural organization of connections between hypothalamus and cerebral cortex Brain research Brain research reviews 24:197-254

1 Rocca MA et al. (2010) Central nervous system dysregulation extends beyond the pain-
2 matrix network in cluster headache Cephalalgia : an international journal of headache
3
4 30:1383-1391 doi:10.1177/0333102410365164
5
6
7 Roosendaal SD, Schoonheim MM, Hulst HE, Sanz-Arigita EJ, Smith SM, Geurts JJG,
8
9 Barkhof F (2010) Resting state networks change in clinically isolated syndrome Brain :
10
11 a journal of neurology 133:1612-1621 doi:Doi 10.1093/Brain/Awq058
12
13
14 Salvador R et al. (2008) A simple view of the brain through a frequency-specific
15
16 functional connectivity measure NeuroImage 39:279-289
17
18 doi:10.1016/j.neuroimage.2007.08.018
19
20
21 Smith SM (2002) Fast robust automated brain extraction Human brain mapping 17:143-
22
23 155 doi:10.1002/hbm.10062
24
25
26 Smith SM, Nichols TE (2009) Threshold-free cluster enhancement: addressing
27
28 problems of smoothing, threshold dependence and localisation in cluster inference
29
30 NeuroImage 44:83-98 doi:10.1016/j.neuroimage.2008.03.061
31
32
33 Sprenger T, Boecker H, Tolle TR, Bussone G, May A, Leone M (2004) Specific
34
35 hypothalamic activation during a spontaneous cluster headache attack Neurology
36
37 62:516-517
38
39
40 Sprenger T et al. (2007) Altered metabolism in frontal brain circuits in cluster headache
41
42 Cephalalgia : an international journal of headache 27:1033-1042 doi:10.1111/j.1468-
43
44 2982.2007.01386.x
45
46
47 Szabo N, Kincses ZT, Pardutz A, Toth E, Szok D, Csete G, Vecsei L (2013) White
48
49 matter disintegration in cluster headache The journal of headache and pain 14:64
50
51 doi:10.1186/1129-2377-14-64
52
53
54 Tajti J, Szok D, Majláth Z, Tuka B, Csáti A, Vécsei L (2015) Migraine and
55
56 neuropeptides Neuropeptides 52:19-30 doi:10.1016/j.npep.2015.03.006
57
58
59
60
61
62
63
64
65

1 Teepker M et al. (2012) Diffusion tensor imaging in episodic cluster headache
2 Headache 52:274-282 doi:10.1111/j.1526-4610.2011.02000.x
3
4 Tian L, Kong Y, Ren J, Varoquaux G, Zang Y, Smith SM (2013) Spatial vs. Temporal
5 Features in ICA of Resting-State fMRI - A Quantitative and Qualitative Investigation
6 in the Context of Response Inhibition PloS one 8:e66572
7 doi:10.1371/journal.pone.0066572
8
9 Tracey I (2008) Imaging pain Br J Anaesth 101:32-39 doi:10.1093/bja/aen102
10
11 Tuka B et al. (2013) Alterations in PACAP-38-like immunoreactivity in the plasma
12 during ictal and interictal periods of migraine patients Cephalalgia 33:1085-1095
13 doi:10.1177/0333102413483931
14
15 van Vliet JA, Vein A, Le Cessie S, Ferrari MD, van Dijk JG, Group DRR (2003)
16 Impairment of trigeminal sensory pathways in cluster headache Cephalalgia 23:414-
17 419
18
19 Xue T et al. (2012) Intrinsic brain network abnormalities in migraines without aura
20 revealed in resting-state fMRI PloS one 7:e52927 doi:10.1371/journal.pone.0052927
21
22 Yang FC et al. (2013) Altered gray matter volume in the frontal pain modulation
23 network in patients with cluster headache Pain 154:801-807
24 doi:10.1016/j.pain.2013.02.005
25
26 Yang FC et al. (2014) Altered hypothalamic functional connectivity in cluster
27 headache: a longitudinal resting-state functional MRI study Journal of neurology,
28 neurosurgery, and psychiatry doi:10.1136/jnnp-2014-308122
29
30 Zou QH et al. (2008) An improved approach to detection of amplitude of low-frequency
31 fluctuation (ALFF) for resting-state fMRI: fractional ALFF Journal of neuroscience
32 methods 172:137-141 doi:10.1016/j.jneumeth.2008.04.012
33
34
35
36
37
38
39
40
41
42
43
44
45
46
47
48
49
50
51
52
53
54
55
56
57
58
59
60
61
62
63
64
65

1
2
3
4
5
6
7
8
9
10
11
12
13
14
15
16
17
18
19
20
21
22
23
24
25
26
27
28
29
30
31
32
33
34
35
36
37
38
39
40
41
42
43
44
45
46
47
48
49
50
51
52
53
54
55
56
57
58
59
60
61
62
63
64
65

Tables

Table 1. Demographic data of the cluster headache patients

Table 2. MNI coordinates (mm) of the increased degree of coactivation in cluster headache patients.

Figure legends

Figure 1. Altered activity of the left mirrored dataset. The **ipsilateral** attention network showed increased activity in the **ipsilateral** superior frontal gyrus and in the **ipsilateral** medio-frontal cortex (a). The increased **activity** was measured at the frequency band 0.08-0.04 Hz ($p < 0.05$) as shown on the power spectrum below. In the cerebellar network increased activity was found in the cerebellar tonsils at the frequency band 0.02-0.01 Hz ($p < 0.05$) as depicted on the power spectrum below. The colorbars above the images represent the p-values. On the power spectrum figures the black curve represents to the CH group mean amplitude, and red curve stands for the healthy group. The green columns displayed the significant differences between the two groups **corrected for multiple comparisons**.

Figure 2. Altered activity of the right mirrored dataset. The **ipsilateral** attention network showed increased activity in the 0.08-0.04 Hz frequency band ($p < 0.01$) in the superior and medial frontal cortex. The analysis revealed decreased activity in the cerebellar network in the cerebellar tonsils (b) at the frequency band 0.02-0.01 Hz ($p < 0.05$). The colorbars represent p-values. The reduced activity is depicted to blue to light blue. The power spectrum of the resting state network's activity is presented below the statistical images. Black curve stands for the CH group mean amplitude, and red curve for the healthy group. The green columns indicate the significant differences between the two groups **corrected for multiple comparisons**.

Figure 3. Correlation was found between cumulative headache days and expression of the resting state activity fluctuations. In the left mirrored dataset, the

1 contralateral attention network showed correlation with the cumulative headache days
2 in the contralateral frontal pole ($p < 0.05$). The right mirrored dataset showed correlation
3
4 in the contralateral attention network (b) near the ipsilateral frontal pole ($p < 0.05$). The
5
6 colorbar represents p-values.
7
8
9

10
11
12
13
14
15
16
17
18
19
20
21
22
23
24
25
26
27
28
29
30
31
32
33
34
35
36
37
38
39
40
41
42
43
44
45
46
47
48
49
50
51
52
53
54
55
56
57
58
59
60
61
62
63
64
65

Figure 1

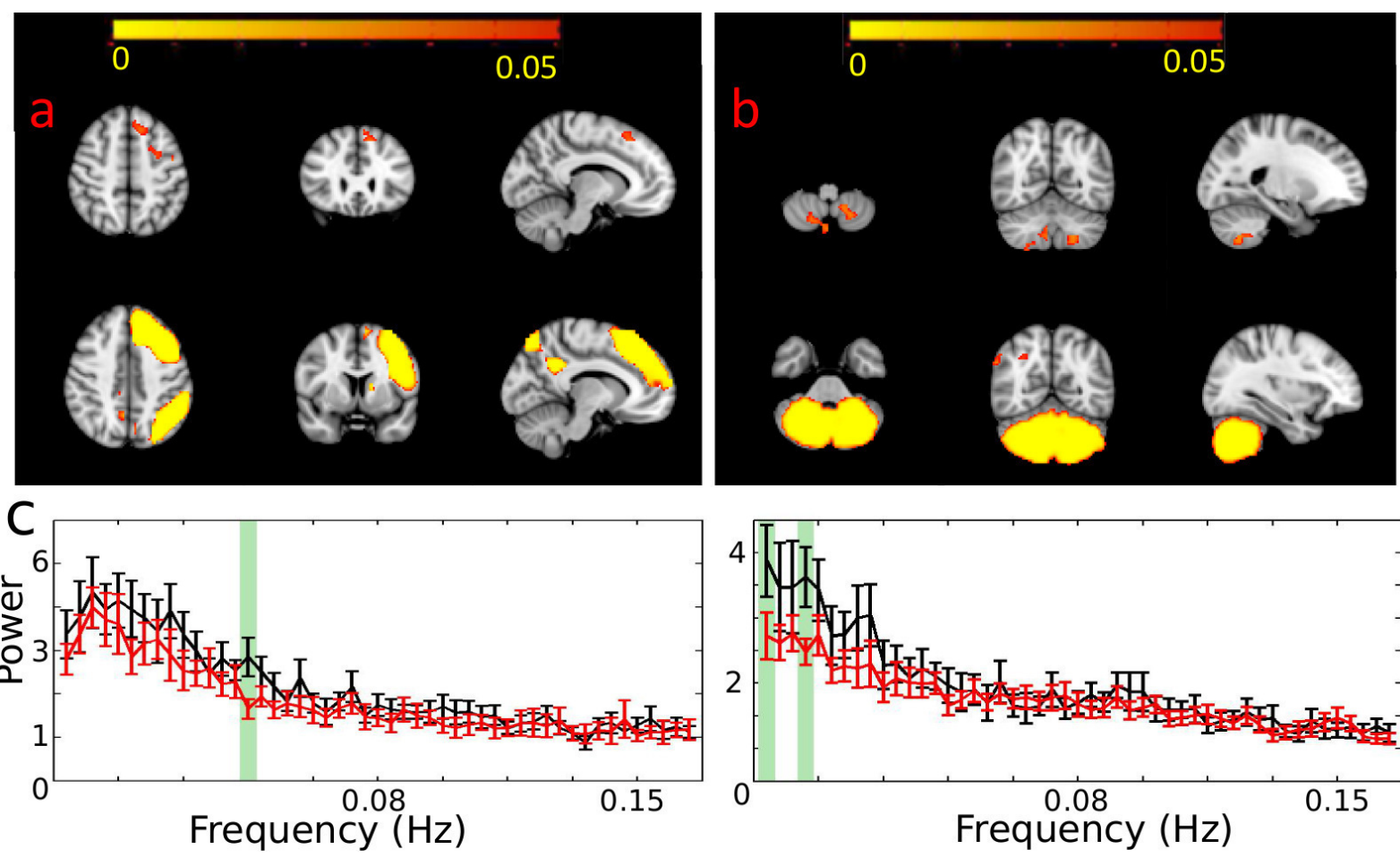


Figure2

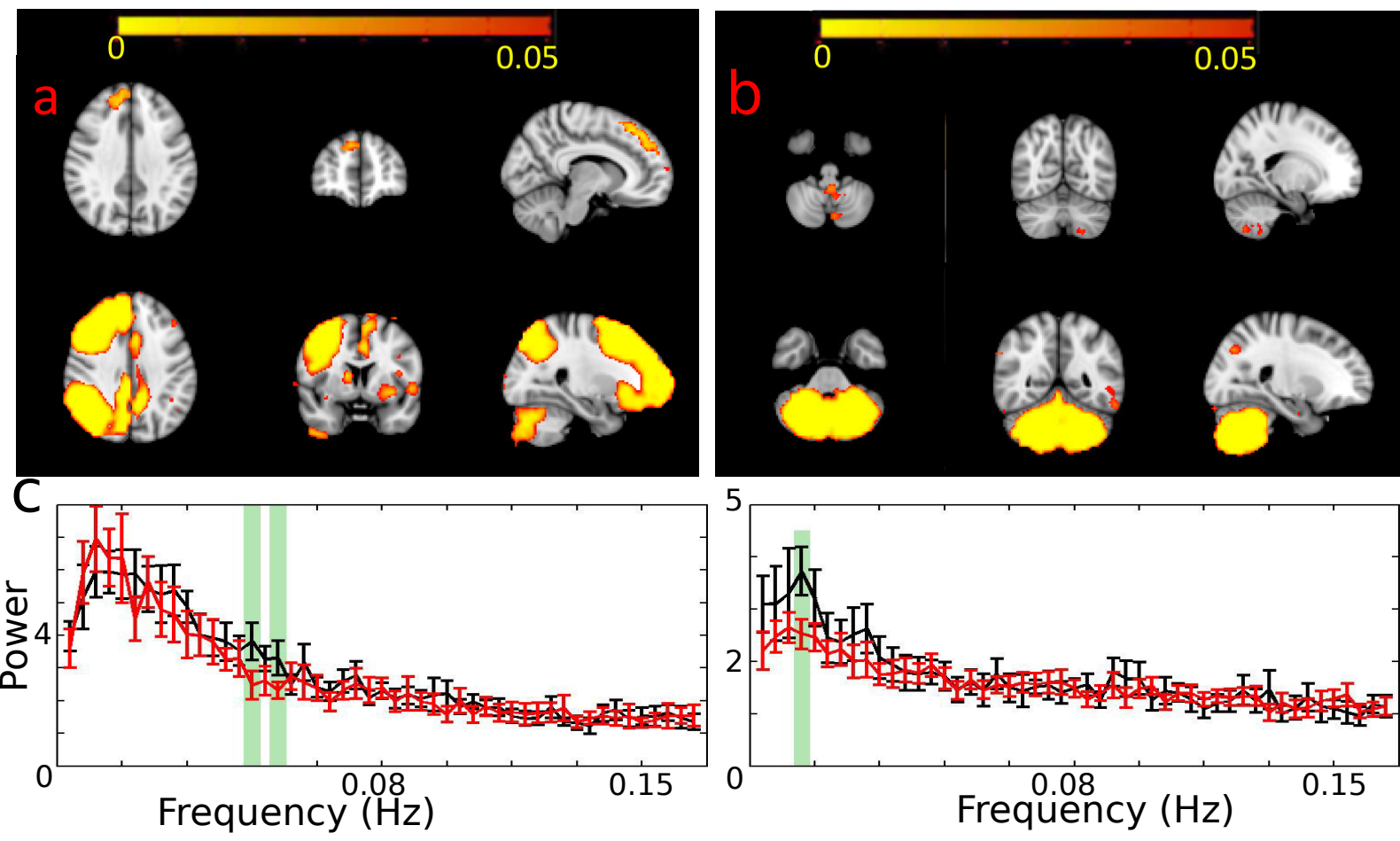


Figure3

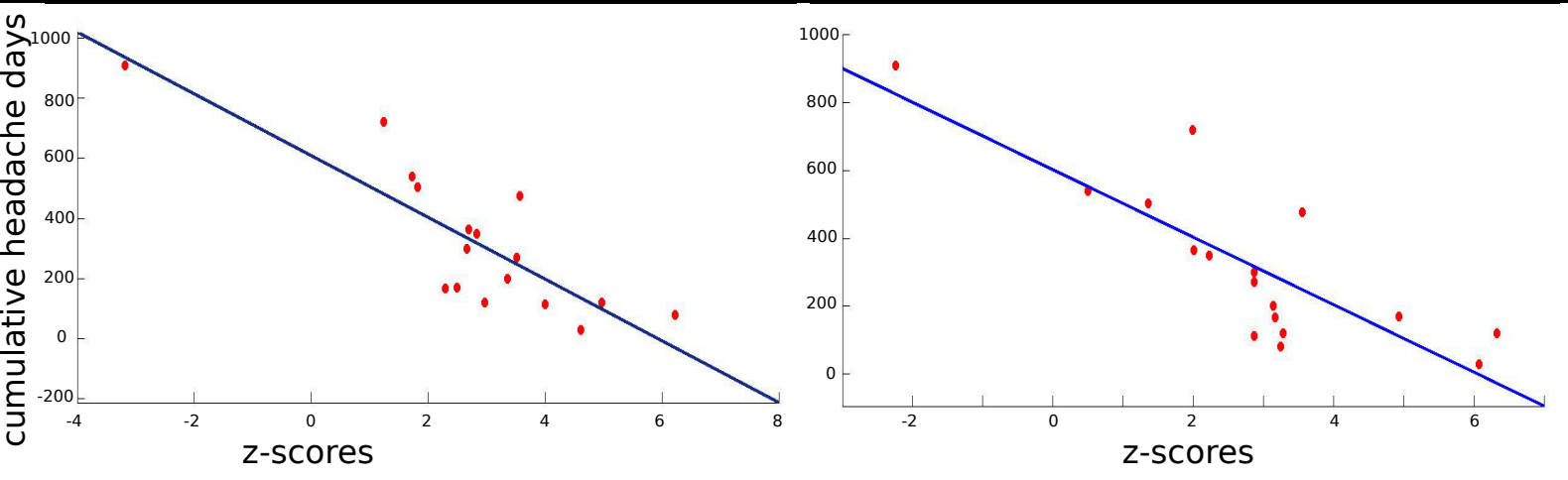
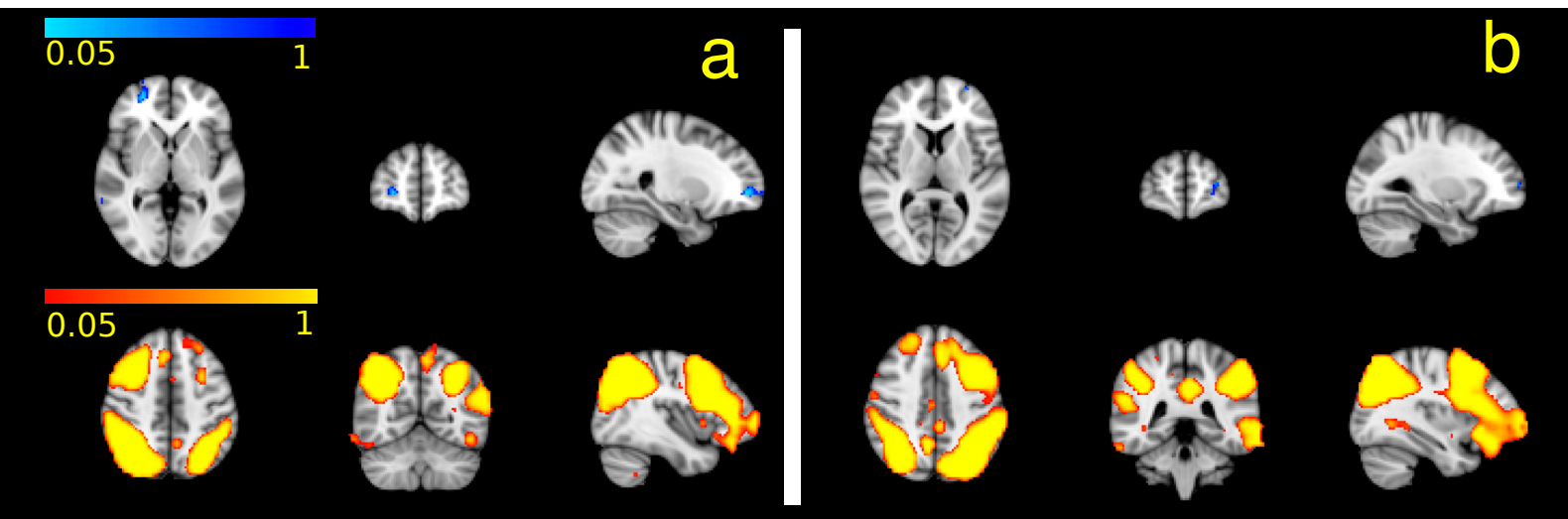
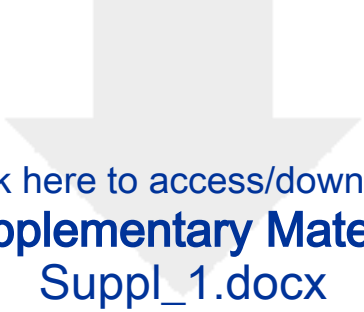


Table1

	controls	patients	p
n	26	17	-
gender (male)	23	15	n.s.
age (years)	37.92±11.55	37,82±11.57	n.s.
handedness (right)	26	17	n.s.
headache side (right)	NA	7	-
Disease duration (years)	NA	7.7±6	-
Average time between bouts (months)	NA	12.6±11.4	-
Average length of bouts (weeks)	NA	4.4±4.1	-
cumulative headache days	NA	319.19±243.3	-

Table2

<i>Left flipped dataset</i>	x (mm)	y (mm)	z (mm)
Left attention network	50	76	64
Cerebellar network	56	33	9
<i>Right flipped dataset</i>			
Right attention network	40	88	53
Cerebellar network	54	31	11



Click here to access/download
Supplementary Material
Suppl_1.docx



Click here to access/download
Supplementary Material
suppl_2_VBM.docx

